51. J. E. Bercaw, paper presented at the Workshop on Homogeneous Catalysis, Royal Netherlands Academy of Arts and Science, Amsterdam, November 1989.
52. P. Hadjiandreou, M. Julemont, Ph. Teyssié, *Macromolecules* **17**, 2456 (1984).
53. T. Yoshimura, T. Masuda, T. Higashimua, *ibid.* **21**, 1899 (1988).
54. T. Masuda, T. Yoshimura, T. Higashimua, *ibid.* **22**, 3805 (1989).
55. T. Otsu, T. Matsunaga, A. Kuriyama, M. Yoshoka, *Eur. Polym. J.* **25**, 643 (1989), and references therein; T. Otsu, M. Yoshida, T. Tazaki, *Makromol. Chem. Rapid Commun.* **3**, 133 (1982).
56. A. Bledzki, D. Braun, K. Titzschkau, *Makromol. Chem.* **184**, 745 (1983), and references therein.
57. D. H. Solomon, E. Rizzardo, P. Cacioli, U.S. Patent 4 581 429 (1986).
58. A procedure for synthesis of peptides by condensation of one amino acid at a time to a chain attached to polystyrene resin.
59. D. A. Tomalia, A. M. Naylor, W. A. Goddard III, *Angew. Chem. Int. Ed. Engl.* **29**, 138 (1990).

DNA: A Model Compound for Solution Studies of Macromolecules

R. PECORA

Well-defined, monodisperse, homologous series of oligonucleotides and DNA restriction fragments may now be produced and used as models of rigid and semirigid rodlike molecules in solution. Information from optical experiments on these model systems aids in the formulation and testing of theories of macromolecular dynamics in both dilute and concentrated solution.

THE PROPERTIES OF POLYMERIC SUBSTANCES ARE DETERMINED by their microscopic molecular structure and dynamics. Many of these properties, especially those that involve motion of the whole or large portions of a polymer chain, are strongly dependent on molecular weight. Most polymeric substances, whether they are solids or liquid dispersions, are polydisperse. They contain polymeric chains of varying degrees of polymerization (molecular weights). Such molecular weight dispersions make it difficult to test microscopic theories of polymer behavior that involve molecular weight–dependent properties. It is highly desirable for fundamental polymer science studies to have sets of well-defined, monodisperse, homologous series of model macromolecules (*1*).

It is generally very difficult to prepare such monodisperse series for synthetic macromolecules, although in some cases relatively narrow dispersions can be made by using "living polymerization" and other methods (*2, 3*). In many cases, fractionation of polydisperse materials can substantially reduce an initial polydispersity, but the resulting material is for many purposes usually still too polydisperse. Very narrowly disperse samples can be prepared of many biological macromolecules and particles (such as virus particles), but it is difficult in most cases to prepare homologous series.

Rigid and semirigid rodlike polymers are of great commercial and biological interest. Some of these polymers, especially the biological ones, are soluble in common solvents. However, even those that are not easily soluble normally must be characterized or processed in solution. For instance, many high-performance polymeric materials, such as Du Pont's Kevlar, are rigid rod polymers. These polymers, in addition to being highly polydisperse, are hard to prepare in high molecular weights and usually cannot be dissolved in noncorrosive solvents. Thus it is difficult to perform careful physicochemical experiments on these systems to characterize their properties (average molecular weights, polydispersity, and so forth) or to test molecular theories of their behavior in solution and in the melt. Their lack of easy solubility also creates problems in processing them into useful materials. Biological examples (usually water soluble) of semirigid rodlike molecules include the rodlike proteins such as collagen, myosin, actin, tubulin, rodlike viruses such as tobacco mosaic virus, fd-virus, and molecules such as the DNAs.

The DNAs present an exception to most of the difficulties of preparing a monodisperse, homologous series of molecules. Very short DNAs ranging from the monomer to about 100 base pairs (bp) in length ("oligonucleotides") may be relatively easily prepared with the aid of DNA synthesizers. Larger molecules may be made by using genetic engineering techniques to prepare appropriate bacterial plasmid DNAs from which monodisperse, blunt-ended fragments may be cut with restriction enzymes ("restriction fragments"). It is also likely that recently developed polymerase chain reaction (PCR) techniques may be used to produce oligonucleotides and fragments even more cheaply than has been previously done. The DNAs are, of course, soluble in water and can be dissolved in other solvents, such as alcohol-water mixtures, to study such phase phenomena as polymer collapse, polymer aggregation, and phase separation. The DNAs are also polyelectrolytes and so they may be used as models for the effects of small ions and the long-range Coulomb force on both the properties of a single polymer chain in solution and the interactions between polyions. The model polyelectrolyte that is most often studied is polystyrene sulfonate, whose polydispersity clouds much of the interpretation of the otherwise sophisticated experiments on it (*4*). Disadvantages of using the DNAs as model molecules include the labor and cost of producing the relatively large amounts needed for certain types of physiochemical measurements. There are also uncertainties expressed by several authors as to the complexity of DNA. For instance, it may be that proteins, either in the natural state or those introduced somewhere in the processing of the DNA, bind to the DNA and cause structural changes in it which affect the properties. Thus, it is possible that one may be studying different materials when ostensibly the same materials are prepared by different procedures (*5*).

In my laboratory a range of DNAs have been used as model systems for macromolecular dynamics in solution. The smaller oligonucleotides (less than about 30 bp in length) are used to test hydrodynamic theories of translational and rotational diffusion for rodlike molecules of relatively low length-to-diameter ratios as well as to extract information about DNA structure and dynamics.

The author is professor of chemistry at Stanford University, Stanford, CA 94305–5080.

Knowledge of overall translational and rotational motion may also be used to help obtain details about the amplitudes and relaxation times of local internal motions within the molecules from various experimental techniques that are sensitive to a combination of overall and local motion [nuclear magnetic resonance (NMR), fluorescence polarization decay, and so forth] (*6–8*). The optical techniques (see below) used to study the overall rotational and translational dynamics are quite sensitive to overall molecular dimensions and may be used to follow processes that result in a change of molecular size or shape (examples for oligonucleotides include B to Z transitions and binding of proteins and anti-cancer drugs).

The restriction fragments (most of which are in the range from several hundred to several thousand base pairs in contour length) are used to model the dynamics of single, semirigid chains in relatively dilute solutions (*9*). In addition to linear double-helical fragments, superhelical and relaxed circles may be studied (*10, 11*). The "flexibility" (defined as the ratio of contour length to persistence length) varies with molecular weight for a given series of molecules (such as the linear ones) and solution conditions. The flexibility of molecules with given molecular weights may be varied by changing solution ionic strength. Dynamic properties that are followed in dilute solution include the translational diffusion coefficients and measures of rotation and large-scale bending modes of the molecules. Total-intensity light scattering and x-ray scattering are used to study structural parameters. The use of DNA restriction fragments avoids many of the problems of data interpretation associated with polydispersity, such as is found in other model polyelectrolytes (such as the polystyrene sulfonates mentioned above). A disadvantage of the restriction fragments is that they are relatively laborious to produce in large amounts without very specialized equipment, so that they have heretofore been used only to study dilute solution properties and only with techniques that require relatively small volumes of sample. The production techniques, while commonplace in biology laboratories, are also generally unfamiliar to polymer scientists.

Optical Techniques for Studying Dynamics

Much of the current work on translational diffusion, rotational diffusion, and long-range intramolecular modes of motion of polymer chains utilizes optical techniques that have been developed in the past few decades. The major methods include several types of light scattering experiments that come under the general heading of dynamic light scattering (DLS). The most common DLS experiment—polarized photon correlation spectroscopy—monitors the temporal fluctuations in the intensity of light scattered from a polymer-containing solution or melt (*12–15*). The basic idea of such an experiment is that the scattered light intensity measured at a photodetector at any given instant is the resultant of the interference of wavelets scattered from different molecules or different parts of a large molecule. This resultant intensity depends on the positions of the scatterers, the scattering angle, and the wavelength of the light used. Since the relative positions of the scatterers changes in a random manner through Brownian motion, the resultant intensity fluctuates in time. The resultant fluctuations in intensity are therefore related to the translational, rotational, and intramolecular motions of the polymer.

The comparison with theory is made by using the intensity autocorrelation function—a statistically averaged moment of the stochastic intensity fluctuation signal. This time correlation function is usually computed on-line during a photon correlation experiment by an autocorrelator—a specially hard-wired computer optimized for quickly computing the function. For the simplest case, a dilute polymer solution studied at low scattering angle, it may be shown that the correlation function is a single exponential decay with a decay constant proportional to the mutual translational diffusion coefficient. At higher scattering angles, the time correlation function often becomes more complex with additional exponentials containing contributions from rotational and long-range intramolecular motions. The photon correlation technique is applicable to dynamical processes with relaxation times greater than about 1 μs, and among its many uses it is one of the major methods of measuring mutual diffusion coefficients of molecules in solution. It has been applied by many workers to the study of high molecular weight DNA (*14, 15*).

Instead of monitoring the intensity fluctuations of the scattered light as in photon correlation spectroscopy, the frequency broadening (spectrum) of the scattered light may be measured by using a Fabry-Perot interferometer—a high-resolution monochrometer (*12*). For the present purposes this method is most useful in measuring the spectrum of the depolarized component of the scattered light (*6–8*). If a molecule is optically anisotropic, the scattered light contains a component with polarization in the scattering plane. This component is broadened by rotational motions of the molecules. The use of Fabry-Perot interferometers is usually limited to the measurement of frequency changes that are greater than a few megahertz because of frequency resolution difficulties. Hence, study of this component is useful for measuring rotational diffusion coefficients of molecules that rotate relatively fast. For oligonucleotides, this includes those less than about 30 bp in length.

Transient electric birefringence (TEB) is another major technique that has been used by several workers over the past decade to study DNA restriction fragments. The most common TEB experiment measures the decay of the birefringence induced in a polymer sample by an external electric field (*16–20*). In a closely related technique, the decay of the electric field-induced dichroism is measured (*21*). This technique can measure rotational as well as long-range internal modes of motion of the molecule. It is not sensitive to translational diffusion and can be used with very small amounts of sample. However, it is generally restricted to samples with relatively low ionic strength because of electrolysis and Joule-heating effects due to the external electric field.

Forced Rayleigh scattering has not yet been used with DNA restriction fragments but has been applied to the study of small fragments produced by sonication of high molecular weight DNA (*22*). This technique should prove useful in studying translational self-diffusion of DNA in concentrated solution and should help elucidate interactions between polymer chains in solution. In this method, also called "holographic grating spectroscopy," a dispersion containing a chromophore-labeled molecule (either natural or synthetically attached) is illuminated by crossed light beams from an exciting laser, which produces a grating of light and dark areas. The chromophore, selected to absorb at the frequency of the exciting laser, is excited in the light areas to produce a refractive index grating that can diffract light. A monitoring laser then illuminates the grating and light is diffracted into a phototube. The exciting laser that produced the grating is then turned off and, if the chromophore has a long-lived excited state, the refractive index grating disappears because of diffusion of the chromophore-containing molecules. The disappearance is followed by measuring the decay of the diffracted intensity (*23, 24*). Fluorescence recovery after photobleaching (FRAP) is a related technique that has been applied to study translational diffusion in concentrated solutions of high molecular weight DNA (*25*). It should be emphasized that these two techniques measure the translational self-diffusion coefficient that in nondilute solutions is different from the mutual diffusion coefficient measured by DLS (*12, 22*).

Rotation and Translation of Oligonucleotides

The rotational and translational diffusion coefficients of oligonucleotides are studied by, respectively, depolarized Fabry-Perot interferometry and polarized photon correlation spectroscopy. In depolarized Fabry-Perot interferometry as applied to oligonucleotides, the scattered light spectrum, after deconvolution from the instrumental line shape, is a Lorentzian whose half-width is six times the molecular end-over-end rotational diffusion coefficient. The polarized photon correlation experiment is done by standard methods and yields the translational diffusion coefficient of the molecule.

The rotational and translational diffusion coefficients of three duplex B-DNA oligonucleotides were measured in my laboratory as well as the rotational diffusion coefficient of a hairpin molecule with an almost spherical shape (*7, 8*). The experiments were done at high ionic strength (50 mM phosphate, 100 mM NaCl, pH = 7), where the Coulomb forces between different molecules are well screened by the small ions. The duplex oligonucleotides that constitute a homologous series have base sequences $d(CG)_n$, where n = 4 (octamer) and 6 (dodecamer), and d[CGTACTAGTTAACTAGTACG] (20 bp). The hairpin molecule d(CGCGTTGTTCGCG) consists of 13 bases (tridecamer) and is folded such that the four bases at each end are paired with each other. The TTGTT sequence forms a loop (*26*):

```
    G
T       T
T       T
  C–G
  G–C
  C–G
  G–C
```

To illustrate the high sensitivity of the technique, the rotational diffusion coefficients of all four oligonucleotides are shown in Fig. 1 as a function of concentration. Note that the molecule with the greatest rotational diffusion coefficient is the hairpin molecule. It rotates faster than the B-form duplexes because of its compact, almost spherical shape. Note also that the measurement of rotational diffusion coefficients is sensitive enough to distinguish between different conformations of oligonucleotides and also between B-form duplexes that differ by only a few base pairs in length. The rotational diffusion coefficients are independent of concentration except at very high concentrations where they decrease sharply, most likely because of aggregation. Of interest for future studies is whether this relative insensitivity to concentration remains at lower ionic strengths, where the Coulomb forces between molecules are likely to be more important.

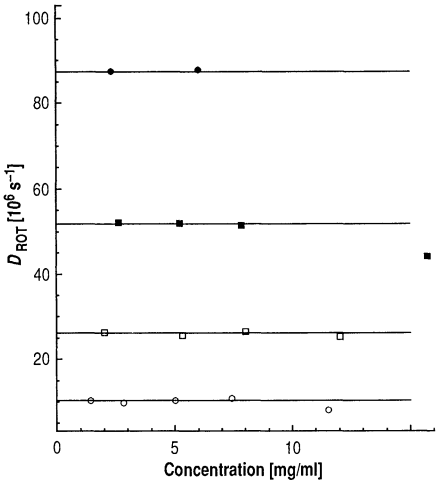

Fig. 1. Rotational diffusion coefficients versus concentration corrected to 20°C for the four oligonucleotides. Plot symbols: (●), tridecamer (hairpin); (■), 8 bp; (□), 12 bp; and (○), 20 bp. The highest concentration points for the 8-bp and 20-bp DNAs are indicative of aggregation. Note that the hairpin (which is almost spherical in shape) has the greatest rotational diffusion coefficient. [Data from (7) and (*8*).]

The translational and rotational diffusion coefficients may be combined to test the consistency of hydrodynamic theories for rotation and translation of short rodlike particles and to obtain a hydrodynamic diameter of DNA in water-based buffer solutions (*7, 8*). The hydrodynamic theories provide quantitative relations between the diffusion coefficients and molecular dimensions. There has been considerable work in recent years in constructing such theories for rodlike molecules with low length-to-diameter ratios. Our studies indicate that the hydrodynamic subunit models of Garcia de la Torre and co-workers give a consistent explanation of the rotational and translational diffusion coefficients of the three duplex B-form oligonucleotides (*27–29*). The data indicate a rise per base pair between 3.4 and 3.5 Å. The three oligonucleotides have a hydrodynamic diameter equal to 20 ± 1.5 Å, an indication of the consistency of the relations through the homologous series. This diameter is about the same as that obtained for the extent of the phosphate groups from x-ray diffraction of solid DNA. It does not include the water of hydration, which is often presumed to rotate with the DNA in solution. Thus, our result is less than the value of 24 to 26 Å usually given for the hydrated diameter of DNA in solution (*30*). This discrepancy may indicate that the water of hydration does not stay on the DNA long enough for the DNA to rotate through an appreciable angle. It is also possibly due to an error in the hydrodynamic relations, which may not be accurate even though they are consistent. The recent theoretical work of Pastor and co-workers (*31*) that uses a more precise model of the surface of the solute molecule may prove useful in elucidating these points. The Pastor model, which has been applied to proteins, but not yet to nucleic acids, takes into account the actual atomic surface area of the solute that is accessible to the solvent.

It should be noted that most studies on the hydrodynamic diameter of DNA use longer oligonucleotides than those described above. The rotational and translational diffusion coefficients of rods are, however, more sensitive to the diameter the shorter the rod.

These methods are applicable to other small rodlike molecules. For instance, the Tirado–Garcia de la Torre relations may be applied to similar optical studies of model compounds (analogs of the repeat units) for rigid rod polymers to obtain "hydrodynamic diameters" that may be then be used to interpret experiments on the polymer.

Dynamics of Restriction Fragments

The strategy in using DNA restriction fragments as model systems is to first use genetic engineering techniques to clone a DNA fragment into a bacterial plasmid DNA (*9*). The bacteria containing the modified plasmids are then allowed to multiply, and the plasmids are extracted. The desired fragment is then cut out of the plasmid with various restriction enzymes, separated from any remaining part of the plasmid that may be present, and prepared for the appropriate experiment. This procedure may be repeated to produce fragments of different lengths. In some cases to increase the yield, more than one copy of a fragment can be inserted into a given plasmid (*9*). These methods have been developed by and are familiar to molecular biologists.

The fragments that are being used in the majority of experiments in our laboratory are 367, 762, 1010, and 2311 bp in contour length. These lengths were chosen so that they could be conveniently studied by both polarized DLS photon correlation spectroscopy and TEB and still be used to elucidate the role of stiffness in the dynamics of the molecules. Superhelical, relaxed circle, and linear B-duplex forms of the 2311-bp fragment have been under study. The 367-, 762-, and 1010-bp fragments are all in the linear B-DNA

Table 1. DNA restriction fragments.

DNA fragment (bp)	Molecular weight* (10^6 daltons)	Contour length† (Å)	L/P‡	Radius of gyration§ (Å)
2311	1.50	7857	16	1044
1010	0.67	3434	7	620
762	0.50	2591	5	510
367	0.24	1248	2.5	291

*Based on 660 daltons per base pair. †A rise per base pair of 3.4 Å is assumed. ‡The ratio of contour length to persistence length for an assumed persistence length of 500 Å. §Calculated for a wormlike coil with a persistence length of 500 Å.

form. Some of the chain parameters of the linear forms are shown in Table 1. The number of persistence lengths per molecule (a measure of the flexibility) and the radius of gyration of the chain are given for the high-salt condition of the DLS experiments, where the persistence length of DNA is 500 Å.

Both DLS (*32*) and TEB (*20, 33–35*) experiments have been performed on the linear forms of all four fragments. The DLS experiments have been done on the relaxed circle form of the 2311-bp fragment (*36*), and both DLS and TEB have been performed on the superhelical form of this same fragment (*11*). The TEB studies were generally done at low ionic strengths (1.5 to 3 mM in sodium) and low concentrations (about 5 to 10 μg ml^{-1}), whereas most of the DLS studies were done at higher ionic strengths (100 mM in sodium) and higher concentrations (about 100 μg ml^{-1}). Note the small amounts of DNA needed for these experiments, especially TEB. Since the persistence length depends on ionic strength, it is likely that in the DLS experiments a fragment of a given molecular weight is more flexible than in the corresponding TEB experiment. The results of DLS experiments at lower ionic strengths (as well as at higher concentrations) would be of much interest.

Both the polarized DLS intensity autocorrelation functions and the TEB decay functions are exponential or sums of exponential decays. The standard methods of analyzing them are embodied in the widely used data analysis programs CONTIN and DISCRETE (*37, 38*). These programs represented an important advance in analyzing data that are not single exponentials. They contain generally accepted algorithms that allow the program to choose relaxation time distributions that are consistent with the DLS or TEB decay functions and the noise in the data.

The TEB experiments on dilute restriction fragment solutions generally show more than one relaxation process, an indication that intramolecular flexing motions contribute directly to the spectra. A plot of the two slowest times versus fragment length extracted from the TEB decays is shown in Fig. 2. Along with the slowest times for the smallest three fragments are shown previous data obtained from the pioneering experiments of Stellwagen (*19*) and Hagerman (*18*) on similarly sized fragments. If it is assumed that the slowest time represents rotational diffusion of the molecule, then the data may be used as a test of theories of rotational motion of semistiff wormlike coils (*39, 40*). Based on the known contour lengths and the measured slowest relaxation time, the theoretical formulas may be used to extract values of the molecular persistence length. This procedure, as pointed out by Hagerman (*18*), gives persistence lengths that vary with fragment length. The persistence lengths at low ionic strengths found by this method vary from about 500 Å for the 367-bp fragment to 1000 Å for the 1010-bp fragment (*20*). It is possible that the persistence length of small fragments may vary with contour length because of electrostatic end effects. There are, however, also indications that the TEB slowest relaxation time is not a pure rotation, but includes contributions from the fluctuations in the molecular shape as the molecule rotates (*35*). The ratio of the slowest relaxation time to that of the next faster mode, as well as the magnitude of the slowest mode, indicates that the largest fragment under these conditions behaves very much like a free-draining Gaussian coil (*41, 42*). The ratio for the smaller fragments at these low salt conditions shows the effects of stiffness.

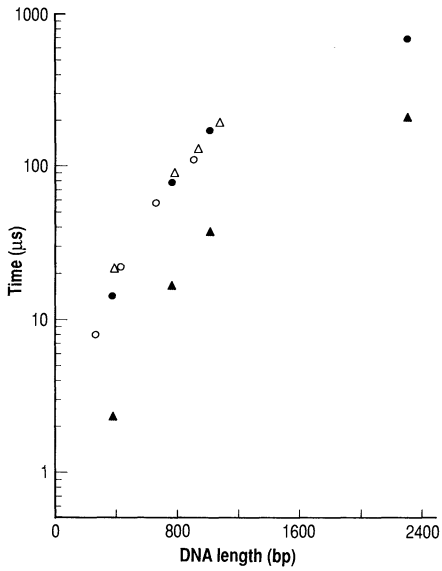

Fig. 2. The two slowest decay times obtained from the transient electric birefringence decay curves for the four restriction fragments. Data from: (▲ and ●), my laboratory (*20*); (○), Hagerman (*18*); and (△), Stellwagen (*19*). The slowest decay time (upper points) is normally interpreted as a rotational relaxation time and the fastest time as a combination of rotation and internal rearrangement. [Reprinted from (*20*) with permission © American Chemical Society.]

At low scattering angles, the time correlation functions from DLS–photon correlation spectroscopy are single exponentials as expected from theory (*12, 43*), but at high angles they are generally composed of two or more significant exponentials. The time constant for the low-angle decay is proportional to the macromolecular mutual diffusion coefficient. (The mutual diffusion coefficient is equal to the self-diffusion coefficient when the macromolecule concentration is low.) The bi- or multiexponential decay function at higher angles is an indication that rotational or intramolecular flexing motions or both are influencing the time correlation functions. With the use of a combination of studies varying the scattering angle and simulations of the relaxation time distribution for models (*32*), it is possible to obtain the translational diffusion coefficient and the relaxation time of the first normal relaxation mode of the fragment.

The translational diffusion coefficients obtained from these studies as well as a comparison with various theories is shown in Table 2. The Yamakawa-Fujii theory, which includes chain stiffness, does the best in predicting the diffusion coefficient, although significant deviations remain, possibly due to the neglect of fluctuations in chain conformation as the molecule translates (*44*).

An example of an analysis performed with the CONTIN program of a DLS time correlation function from the 762-bp DNA fragment

Table 2. Translational diffusion coefficients. The experimental values (Expt.) are from (*32*). The nondraining Gaussian coil values were calculated with the values for the radius of gyration given in Table 1. The rigid rod values were calculated by using the contour length given in Table 1 as the rod length. The Yamakawa and Fujii values were calculated with the formula given in (*44*) and the parameters given in Table 1.

DNA length (bp)	Translational diffusion coefficient (10^{-8} cm^2 s^{-1})			
	Expt.	Nondraining Gaussian coil	Rigid rod	Yamakawa and Fujii
2311	4.56 ± 0.13	3.04	3.23	4.31
1010	7.15 ± 0.19	5.11	6.29	7.59
762	9.05 ± 0.11	6.21	7.84	9.27
367	15.8 ± 0.47	10.9	13.2	15.7

is shown in the middle portion of Fig. 3. The scattering angle is 123°. The plot shows the fraction of the scattered correlation function (actually the scattered electric field correlation function) that relaxes with a given apparent hydrodynamic radius. The hydrodynamic radius R_h is simply defined in terms of the reciprocal of the apparent diffusion coefficient D through the Stokes-Einstein relation:

$$R_h = k_B T/6\pi\eta D$$

where k_B is Boltzmann's constant, T is the temperature in Kelvin, and η is the solvent viscosity. The large peak with ~90% of the scattered intensity represents the translational diffusion of the molecule. The peak with ~9% of the area represents both translational diffusion of the molecule and a further, faster contribution from rotational or long-range internal motion of the chain or both. It is from this peak that the value of for the longest mode internal relaxation time of the chain may be obtained. The third peak at very small hydrodynamic radius (not included in the percentage calculations of the other peaks) is less than a few percent of the total relaxation function and is possibly an artifact of the data analysis method. A peak of this type is often observed in both simulated and real data for a wide variety of systems at the low R_h end of the CONTIN window. If the CONTIN window is moved to even lower R_h values, this peak usually follows it.

Also shown in Fig. 3 are CONTIN analyses of calculated correlation functions for a rigid rod model (top) and a free-draining Gaussian coil model (bottom) of this fragment. These models have as inputs the measured value of the translational diffusion coefficient from low-angle DLS (for both the rod and coil), the theoretical radius of gyration for a wormlike coil based on the persistence length (coil model), and the length and rotational diffusion coefficient calculated for a straight rod with the given number of base pairs (rod model). Note that the free-draining Gaussian coil distribution gives good agreement with experiment.

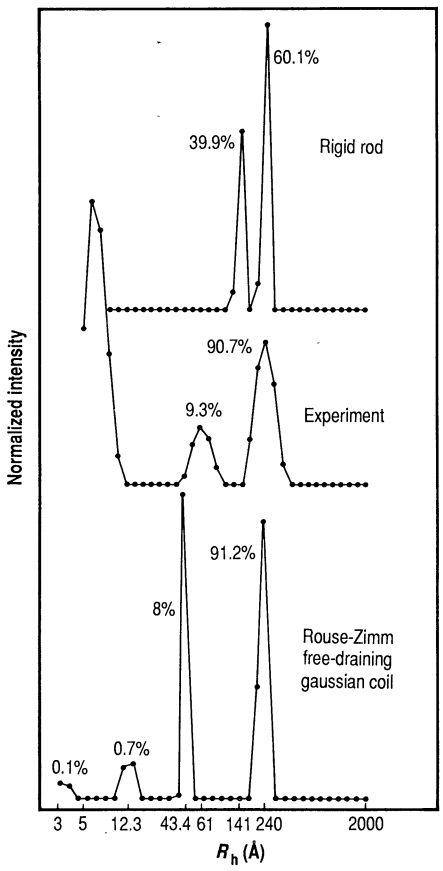

Fig. 3. Distribution of hydrodynamic radii (proportional to the relaxation times) from CONTIN analysis of the DLS time correlation function for the 762-bp linear, B-DNA restriction fragment (middle; charge times radius of gyration equals 1.5). Also shown are CONTIN analyses of calculated time correlation functions for a rod model (top) and free-draining Gaussian coil model (bottom) of the same fragment. [Reprinted from (*32*) with permission © American Chemical Society.]

In general the DLS experiments for all four restriction fragments give translational diffusion coefficients that are in reasonable agreement with those predicted by the Yamakawa-Fujii theory for translational diffusion of wormlike chains. The internal times for the longest three fragments (the 367-bp fragment is too small to measure internal times by DLS), however, are in best accord with those predicted by the free-draining Gaussian coil model with input parameters consisting of the experimental translational diffusion coefficient and the radius of gyration of a wormlike coil with the persistence length and contour length of the given DNA. In fact, as illustrated in Fig.3, the entire relaxation time distribution is well approximated by this model. This apparent agreement with the free-draining model is likely to be the result of an approximate cancellation of effects due to hydrodynamic interaction and chain stiffness, both of which are included in free-draining Gaussian coil model calculations in a rather indirect way (*45*). The TEB studies show similar agreement with the free-draining model for the 2311-bp fragment, but, as mentioned above, the shorter fragments show significant deviations from free-draining Gaussian coil behavior. These deviations are most likely due to the TEB studies being done at lower ionic strength, where the persistence length of DNA is higher and the molecules are stiffer.

Prospects

Only relatively few experiments have been done in which well-defined DNA are used to model the behavior of stiff and semistiff rodlike molecules in solution. Most data to date have been obtained in the dilute solution regime. Even in this regime, there is still no satisfactory theory of the dynamics of semistiff molecules that incorporates in a unified way the translational, rotational, and long-range intramolecular degrees of freedom, although there are several intriguing models (*46, 47*). Other aspects of the dilute solution behavior, including polyelectrolyte effects, transitions between different helical forms of DNA, and chain collapse effects could be profitably studied (*48–50*).

Some experiments with restriction fragments and oligonucleotides have been done on concentration effects on the dynamics in the dilute regime, but usually not in a systemic manner over an entire homologous series (*25, 32*). Pioneering experiments have, however, been done in this and in more concentrated regimes in which small fragments produced by sonication of high molecular weight DNA have been studied (*22, 51–55*). Ultimately, when the costs of producing larger amounts of fragments are overcome, experiments can be done with monodisperse DNA in these more concentrated regimes. Additional techniques that use relatively large volumes of solution such as viscoelastic relaxation and dispersion also could be used. A problem of particular interest is possible solution ordering at low ionic strengths (*52, 56*) and the gel and cholesteric liquid-crystal phases formed under some conditions (*53, 57*).

REFERENCES AND NOTES

1. M. Doi and S. F. Edwards, *The Theory of Polymer Dynamics* (Clarendon, Oxford, 1986); O. W. Webster, *Science* **251**, 887 (1991).
2. M. Szwarc, M. Levy, R. Milkovich, *J. Am. Chem. Soc.* **78**, 2656 (1956).
3. T. Kitano, T. Fujimoto, M. Nagasawa, *Polymer J.* **2**, 153 (1977).
4. V. Degiorgio *et al.*, *Phys. Rev. Lett.* **64**, 1043 (1990).
5. V. A. Bloomfield, in *Dynamic Light Scattering: Applications of Photon Correlation Spectroscopy*, R. Pecora, Ed. (Plenum, New York, 1985).
6. W. Eimer, thesis, Bielefeld University, Bielefeld, Germany (1987).
7. _____, J. R. Williamson, S. G. Boxer, R. Pecora, *Biochemistry* **29**, 799 (1990).
8. W. Eimer and R. Pecora, *J. Chem. Phys.*, in press.
9. R. J. Lewis, J. H. Huang, R. Pecora, *Macromolecules* **18**, 1530 (1985).
10. G. Voordouw, Z. Kam, N. Borochov, H. Eisenberg, *Biophys. Chem.* **8**, 71 (1978).
11. R. J. Lewis, J. H. Huang, R. Pecora, *Macromolecules* **18**, 944 (1985).
12. B. J. Berne and R. Pecora, *Dynamic Light Scattering* (Wiley-Interscience, New York, 1976).

13. R. Pecora, Ed., *Dynamic Light Scattering: Applications of Photon Correlation Spectroscopy* (Plenum, New York, 1985).
14. K. S. Schmitz, *An Introduction to Dynamic Light Scattering by Macromolecules* (Academic Press, New York, 1990).
15. J. M. Schurr and K. S. Schmitz, *Annu. Rev. Phys. Chem.* **37**, 271 (1986).
16. J. G. Elias and D. Eden, *Macromolecules* **14**, 410 (1981).
17. _____, *Biopolymers* **20**, 2369 (1981).
18. P. J. Hagerman, *ibid.*, p. 1503; *ibid.* **22**, 811 (1983).
19. N. C. Stellwagen, *ibid.* **20**, 399 (1981).
20. R. J. Lewis, R. Pecora, D. Eden, *Macromolecules* **19**, 134 (1981).
21. S. Diekmann *et al.*, *Biophys. Chem.* **15**, 263 (1982).
22. L. Wang, M. M. Garner, H. Yu, *Macromolecules*, in press.
23. F. Rondelez, in *Laser Scattering in Fluids and Macromolecular Solutions*, V. Degiorgio, Ed. (Plenum, New York, 1980).
24. H. Hervet, W. Urbach, F. Rondelez, *J. Chem. Phys.* **68**, 2725 (1978).
25. B. A. Scalettar, J. E. Hearst, M. P. Klein, *Macromolecules* **22**, 4550 (1989).
26. J. R. Williamson and S. G. Boxer, *Biochemistry* **28**, 2819 (1989).
27. M. M. Tirado and J. Garcia de la Torre, *J. Chem. Phys.* **71**, 2581 (1979); *ibid.* **73**, 1986 (1980).
28. M. M. Tirado, M. C. Lopez Martinez, J. Garcia de la Torre, *ibid.* **81**, 2047 (1984).
29. J. Garcia de la Toree *et al.*, *Biopolymers* **23**, 611 (1984).
30. M. Mandelkern *et al.*, *J. Mol. Biol.* **152**, 153 (1981).
31. R. M. Venable and R. W. Pastor, *Biopolymers* **27**, 1001 (1988).
32. S. S. Sorlie and R. Pecora, *Macromolecules* **21**, 1437 (1988); *ibid.* **23**, 487 (1990).
33. R. J. Lewis, thesis, Stanford University, Stanford, CA (1985).
34. _____, D. Eden, R. Pecora, *Macromolecules* **20**, 2579 (1987).
35. R. J. Lewis, S. A. Allison, D. Eden, R. Pecora, *J. Chem. Phys.* **89**, 2490 (1988).
36. J. Seils and R. Pecora, unpublished results.
37. S. W. Provencher, *Comput. Phys. Commun.* **27**, 213, 229 (1982).
38. S. E. Bott, thesis, Stanford University, Stanford, CA (1984).
39. P. J. Hagerman and B. H. Zimm, *Biopolymers* **20**, 1481 (1981).
40. T. Yoshizaki and H. Yamakawa, *J. Chem. Phys.* **81**, 982 (1984).
41. B. H. Zimm, *ibid.* **24**, 269 (1956).
42. H. Yamakawa, *Modern Theory of Polymer Solutions* (Harper and Row, New York, 1971).
43. R. Pecora, *J. Chem. Phys.* **40**, 1604 (1964); *ibid.* **48**, 4126 (1968); *ibid.* **49**, 1032 (1968).
44. H. Yamakawa and M. Fujii, *ibid.* **64**, 5222 (1976).
45. S. A. Allison, S. S. Sorlie, R. Pecora, *Macromolecules* **23**, 1110 (1990).
46. D. B. Roitman and B. H. Zimm, *J. Chem. Phys.* **81**, 6333 (1984); *ibid.*, p. 6348; D. B. Roitman, in *Rotational Dynamics of Small and Macromolecules*, Th. Dorfmüller and R. Pecora, Eds. (Springer, Heidelberg, 1987).
47. S. R. Argon and R. Pecora, *Macromolecules* **18**, 1868 (1985); S. R. Aragon, *ibid.* **20**, 370 (1987).
48. C. B. Post and B. H. Zimm, *Biopolymers* **21**, 2123 (1982); *ibid*, p. 2139.
49. A. A. Brian, H. L. Frisch, L. S. Lerman, *ibid.* **20**, 1305 (1981).
50. J. Widom and R. L. Baldwin, *ibid.* **22**, 1595 (1983); *ibid.*, p. 1621.
51. T. Hard and D. R. Kearns, *ibid.* **25**, 1519 (1986).
52. W. Fulmer, J. A. Benbasat, V. A. Bloomfield, *ibid.* **20**, 1147 (1981).
53. M. G. Fried and V. A. Bloomfield, *ibid.* **23**, 2141 (1984).
54. T. Nicolai and M. Mandel, *Macromolecules* **22**, 438 (1989); *ibid.*, p. 2348.
55. H. Tj. Goinga and R. Pecora, unpublished results.
56. S. F. Schulz *et al.*, *J. Chem. Phys.* **92**, 7087 (1990).
57. T. E. Strzelecka and R. L. Rill, *J. Am. Chem. Soc.* **109**, 4513 (1987); *Biopolymers* **30**, 57 (1990).
58. Supported by the National Science Foundation and by the NSF-MRL program through the Center for Materials Research at Stanford University. I wish to thank my past and present collaborators on this work. They are cited in the references.

Polymer-Polymer Phase Behavior

FRANK S. BATES

Different polymers can be combined into a single material in many ways, which can lead to a wide range of phase behaviors that directly influence the associated physical properties and ultimate applications. Four factors control polymer-polymer phase behavior: choice of monomers, molecular architecture, composition, and molecular size. Current theories and experiments that deal with the equilibrium thermodynamics and non-equilibrium dynamics of polymer mixtures are described in terms of these experimentally accessible parameters. Two representative molecular architectures, binary linear homopolymer mixtures and diblock copolymers, exhibiting macrophase separation and microphase segregation, respectively, are examined in some detail. Although these model systems are fairly well understood, a myriad of mixing scenarios, with both existing and unrealized materials applications, remain unexplored at a fundamental level.

MIXING, ALLOYING, AND BLENDING ARE FAMILIAR TERMS that describe the process of combining two or more elements, compounds, or molecular species into a single product. The associated mechanical, chemical, electrical, and various other properties are largely determined by the resulting phase behavior. For example, copper and zinc form a single solid phase known as brass that is mechanically superior to either constituent alone. Nonequilibrium microstructured phases in steel, produced by adding carbon and other elements to iron, can impart exceptional strength and hardness. Mixtures of oil and water that normally macroscopically phase separate can be finely dispersed by the addition of small amounts of surfactant, which can lead to gross changes in wetting and flow properties. All of these effects can be obtained with polymer-polymer mixtures, sometimes with the use of a single pair of monomeric building blocks. Such a diverse range of phase behaviors and the accompanying breadth of materials applications stem from the unparalleled range of molecular architectures that can be realized with polymers.

This article reviews polymer-polymer phase behavior beginning with a discussion of molecular architecture. Subsequently, overviews of equilibrium thermodynamics and phase separation dynamics are presented. Attention is restricted to binary combinations of amorphous polymers since most of the fundamental theoretical and experimental efforts have focused on these materials; crystalline polymers and multicomponent mixtures fall outside the scope of this article. The subject matter can be further subdivided into two categories, homopolymer mixtures and block copolymers. In each, discussion is focused on the most basic molecular architectures, that is, linear homopolymers and diblock copolymers, since these have been studied most intensely. A summary and brief comment regarding future prospects for this field are presented in the final section.

Molecular Architecture

The number of molecular configurations available to a pair of chemically distinct polymer species (here we define a polymer as a

The author is in the Department of Chemical Engineering and Materials Science, University of Minnesota, Minneapolis, MN 55455.